



Dynamic Response of GFRP-RC Moment-Resisting Frames

Shervin K. Ghomi¹, Ehab El-Salakawy²

¹ Ph.D. Candidate, Department of Civil Engineering, University of Manitoba - Winnipeg, MB, Canada.

² Professor, Department of Civil Engineering, University of Manitoba - Winnipeg, MB, Canada.

ABSTRACT

In the last few decades, non-corrodible glass fibre reinforced polymers (GFRP) have been introduced as an alternative to conventional steel reinforcement in reinforced concrete (RC) structures to mitigate structural strength and serviceability loss due to corrosion of steel in harsh environment. Up to date, many researchers have been involved in investigating various aspects of the behaviour of GFRP-RC elements. One of the areas that has gained some attentions recently, is the use of GFRP materials in seismic regions. Some researchers have investigated the seismic behaviour of various GFRP-RC elements in moment-resisting frames such as columns, beam-columns and beam-column-slab assemblies under seismic-simulated loads. However, research data for dynamic response of an entire GFRP-RC moment frame is scarce. To address this gap, a series of nonlinear finite element models were generated to simulate the dynamic response of an arbitrary five-story moment-resisting frame using SAP2000 software. The main parameters of the study were the type of reinforcement (GFRP and steel) and the presence of cast-in-situ slabs. The lateral load-displacement response of a series of full-scale GFRP-RC and steel-RC beam-column and beam-column-slab connections, experimentally tested by the authors, were used to define the seismic characteristics of the modelled frames. The response of the frames is discussed in terms of maximum lateral deformations and residual damage in the structural elements. The results indicated that including the effect of cast-in-situ slabs to the dynamic analysis, in terms of lateral load-displacement response and mass, can significantly influence the response of moment frames. Moreover, it was concluded that replacing steel reinforcement with GFRP can reduce the magnitude of residual damage after an earthquake event.

Keywords: GFRP-RC, Moment frames, Dynamic response, Beam-columns, Beam-column-slabs, Seismic.

INTRODUCTION

Replacing conventional steel reinforcement with non-corrodible alternatives has been sought by engineers and researchers to eliminate the adverse effects of steel corrosion on the integrity and serviceability of reinforced concrete (RC) structures. Fiber reinforced polymers (FRPs) have been introduced as a successful alternative reinforcement with the added advantage of higher strength-to-weight ratio compared to the conventional steel, offering easier handling and caging process.

However, FRP materials possess different mechanical properties compared to that of conventional steel, which necessitates re-investigation of the behaviour of various concrete elements reinforced with such materials. Among various FRP materials commonly available to the construction industry, Glass-FRP (GFRP) is of particular interest, due to its relatively lower cost compared to other types of fibres.

Since the introduction of GFRP materials to the construction industry, many researchers have been involved in investigating various aspects of the performance of GFRP-RC elements. One of the areas that has been getting some attentions lately is the seismic performance of GFRP-RC moment-resisting frames (MRFs). Few researchers focused on the seismic behaviour of key structural elements in MRFs such as columns [1-3] and beam-column connections [4-8]. Results from these pioneer investigations on the seismic behaviour of GFRP-RC beam-column joints [4-8] concluded that the linear elastic characteristic of GFRP reinforcement results in lack of ductility and lower energy dissipation of GFRP-RC structures.

Moreover, relatively lower modulus of elasticity of GFRP material, compared to that of steel (60 GPa vs. 200 GPa), results in lower lateral stiffness of GFRP-RC frames compared to their steel-RC counterparts, which, could increase the maximum lateral displacement of these structures in a seismic event.

However, on the other hand, the lower stiffness of GFRP-RC frames reduces their natural frequency, which in turn lowers the base design force of these structures and, adversely, reduces their maximum lateral deformation [9]. Furthermore, it has been reported [5,6,8] that GFRP-RC frames can undergo big lateral deformations with insignificant residual damage. This feature allows these structures to resist bigger deformation limits compared to that of steel-RC structures during an earthquake.

Therefore, replacing steel reinforcement with GFRP, could affect various characteristics of MRFs, which could potentially result in opposite effects on the seismic performance of the structures. Up to date, the majority of research was focused on seismic performance of isolated elements in GFRP-RC moment frames, while there is limited data available on the integral performance of an entire GFRP-RC frame under dynamic loads. Due to lack of research data, current codes and guidelines for design of FRP-RC structures such as CAN/CSA-S806-12 [10] and ACI 440.1R-15 [11] do not have a comprehensive seismic section.

This program is aiming at studying the effect of replacing steel reinforcement with GFRP materials on the seismic response of moment-resisting frames. An analytical finite element model (FEM) was constructed using the commercial software SAP2000 [12] to simulate the dynamic response of an arbitrary five-story moment-resisting frame under reversal cyclic loading.

To simulate the dynamic response of an MRF, understanding the seismic performance of beam-column connections, as the key elements in shaping the dynamic characteristics of moment frames is essential. In this program, test results obtained from previous experimental studies on the seismic behaviour of interior beam-columns and beam-column-slabs, conducted by the authors, were used to calculate and define non-linear lateral load-displacement relationships of the modelled frames.

The main studied parameters included reinforcing materials (steel or GFRP) and presence of cast-in-situ slabs. The importance of including the effect of slabs on the seismic performance of steel-RC moment frames is well established [13-15]. Similarly, results of the experimental investigations conducted by the authors on the effect of slabs on the performance of GFRP-RC beam-column connections, confirmed the importance of the slab contribution in the seismic performance of GFRP-RC frames.

SUMMARY OF EXPERIMENTAL PROGRAM

Test Specimens

A comprehensive experimental program investigating the seismic behaviour of GFRP-RC beam-column and beam-column-slab connections has been conducted by the authors. Among twenty full-scale specimens, four specimens, two beam-column and two beam-column-slab assemblies, are considered in the current program. Figure 1-a shows geometry and dimensions of the beam-column specimens. One of the beam-column specimens (designated as BC-S) was reinforced entirely with conventional steel reinforcement, while the other one (designated as BC-G) was completely reinforced with GFRP bars and stirrups. The reinforcement in Specimens BC-S and BC-G was proportioned for identical bending moment capacity of the main beam.

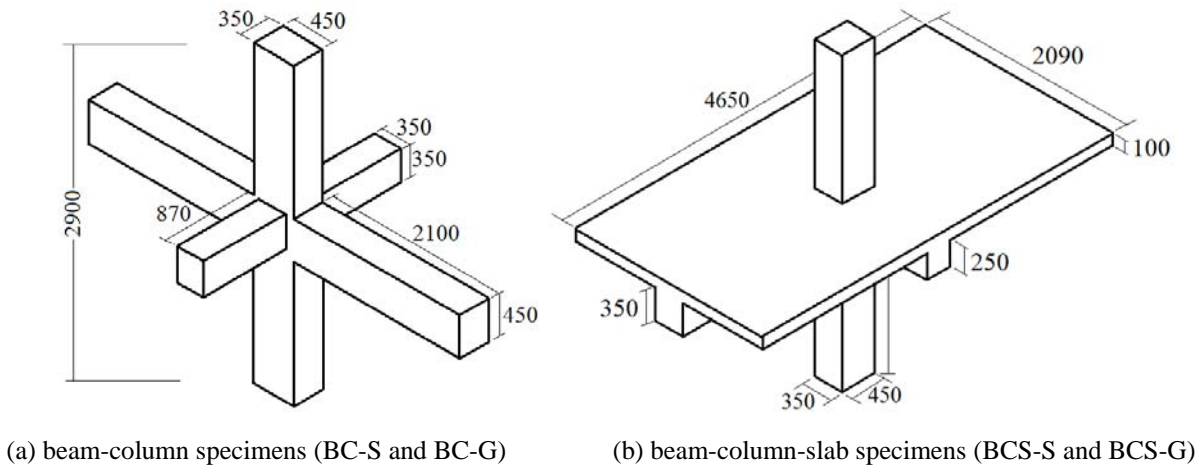


Figure 1. Geometry and dimensions of test specimens (mm).

Similarly, the two beam-column-slab specimens were identical in geometry (shown in Figure 1-b) but were reinforced with different materials (steel and GFRP). The GFRP-RC and steel-RC beam-column-slab specimens are designated as BCS-G and BCS-S, respectively. Properties of the test specimens are summarized in Table 1.

The specimens were isolated from an arbitrary moment frame at the assumed points of contra-flexure at mid-height of the columns and mid-span of the beams. The lateral load-displacement response obtained from the full-scale testing is adapted in the current program to define the nonlinear dynamic response of the analytical models.

Table 1. Properties of test specimens.

Specimens	Beam Flexural Capacity ¹ (kN.m)	Column-to-Beam Flexural Ratio	Concrete Strength (MPa)
BC-G	330	0.98	49
BC-S	361	1.16	56
BCS-G	333	0.99	50
BCS-S	321	1.30	55

¹Capacity without contribution of slabs

Ready mix concrete with target 28-day compressive strength of 45 MPa was used for construction of the test specimens. The actual concrete strength at the day of testing was measured through testing of standard cylinders and are reported in Table 1. Regular deformed CSA Grade G400 steel bars were used in the steel-RC specimens. The yield strength and modulus of elasticity of the steel longitudinal bars were obtained through standard tension test and are included in Table 2. Sand-coated GFRP bars were used for the GFRP-RC specimens. The mechanical properties of the GFRP reinforcement were provided by the manufacturer [16] and are summarized in Table 2.

Table 2. Properties of reinforcement.

Reinforcement	GFRP Tensile Strength, Steel Yield Strength (MPa)	Modulus of Elasticity (GPa)
Beam Longitudinal GFRP Bars	1184	62.6
Slab Longitudinal GFRP Bars	1312	65.6
GFRP Stirrups ¹	1019	50.0
Steel Bars and Stirrups	438	184.8

¹Properties of the straight portion of bent bars

Test Procedure

The specimens were tested under reversal lateral loading to measure their lateral load-displacement response. Figure 2 shows the test set-up used in the program. The reversal cyclic loading was applied to the tip of the columns by means of a hydraulic actuator, mounted on a strong wall. Tips of the main beams were attached to the strong floor with a double-hinged hollow structural section (HSS) to simulate a roller boundary condition by allowing rotation and horizontal movement of the beams, while restricting the vertical displacements.



Figure 2. Test set-up.

The columns were sitting on a hinge, connected to the strong floor by four post-tensioned dywidag bars. The actuator was attached to the columns by a swivel to eliminate exertion of bending moments to the column tips while loading. The swivel on top and the hinge at the bottom of the columns were to simulate the hinge boundary condition at the points of contra-flexure.

The columns were under constant axial load during testing by means of a hydraulic jack. The jack was attached to a stiff steel reaction beam on top of the specimens, connected to the strong floor by means of two long double-hinged HSSs. This set-up allowed for free movement of the stiff beam along with the columns as the actuator applied reversal loading.

The reversal cyclic loading was in displacement-controlled mode measured by the lateral drift ratios, defined as the ratio of column tip displacement (actuator's stroke) to the column length. The lateral loading protocol was adapted from ACI 374.1-05 [17] and was applied in a series of loading steps gradually increasing in the magnitude of drift ratio. For the scope of this document, the response of the specimens from 0% to 5% drift ratio as shown in Figure 3 is considered. As shown in the figure, each loading step consisted of three identical loading cycles.

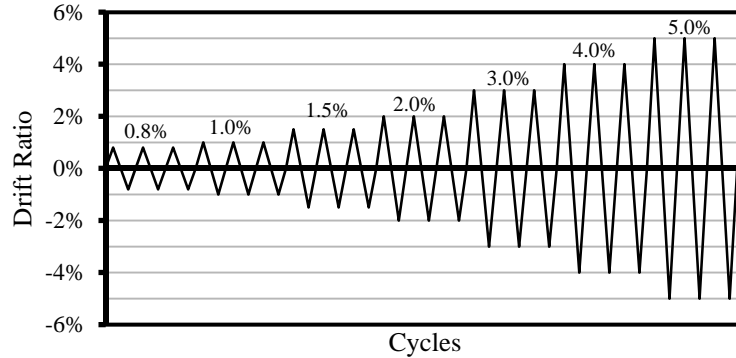


Figure 3. Loading procedure.

ANALYTICAL PROGRAM

In order to investigate the dynamic response of GFRP-RC moment frames, a non-linear finite element model was created to simulate the response of a series of arbitrary 5-story moment-resisting frames under the ground acceleration history recorded for the 1999 Chi-Chi, Taiwan earthquake. In this program, the recorded ground acceleration was scaled to represent a seismic event with peak ground acceleration (PGA) of approximately 0.15g (Figure 4). The finite element program SAP2000 [12] was used to perform the non-linear dynamic analysis.

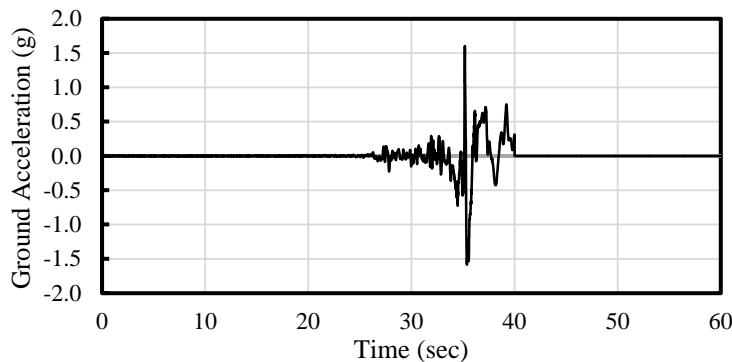


Figure 4. Ground acceleration used for dynamic analysis.

Figure 5 shows the geometry and analytical model of the arbitrary frames under investigation. Four frames were considered, each corresponding to one of the test specimens. For simplicity, the beams were modeled with relatively high stiffness to limit the degrees of freedom to only horizontal displacement in each story. Each column was modeled as a nonlinear link with lateral load-displacement properties obtained from each test specimen. Therefore, the beam-column joints in the modeled frames were assumed to have the same lateral load-displacement response as their corresponding test specimens. Nonlinear links with built-in “Degrading” hysteresis model in the software was used to model the beam-columns. A joint mass equal to the self-weight of each specimen (3,300 kg and 5,600 kg for beam-column and beam-column-slab specimens) was assigned to each node in the analytical model.

It should be mentioned that by considering only the beams and columns in the modeled frames corresponding to Specimens BC-S and BC-G, the model does not represent an actual moment-resisting frame since the effect of slabs is not included. However, the main purpose of the analytical frames with only beams and columns is to serve as a control for investigating the effect of slabs on the dynamic performance of MRFs.

To validate the analytical model, the lateral displacement response of the links under a cyclic lateral load identical to those obtained from the experimental tests was recorded. Figure 6 compares the experimental hysteresis loops of the specimens with the response obtained from their corresponding links in the computer model. As shown in the figure, the responses were in good agreement, therefore the model was assumed valid for conducting further dynamic analysis.

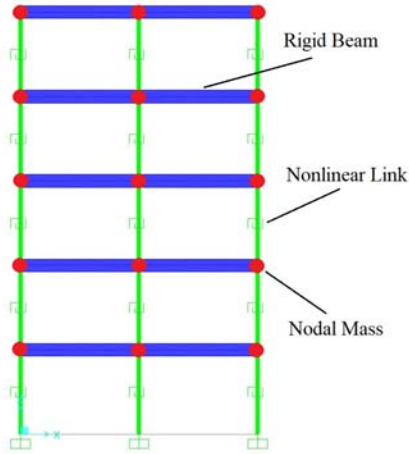


Figure 5. FEM model.

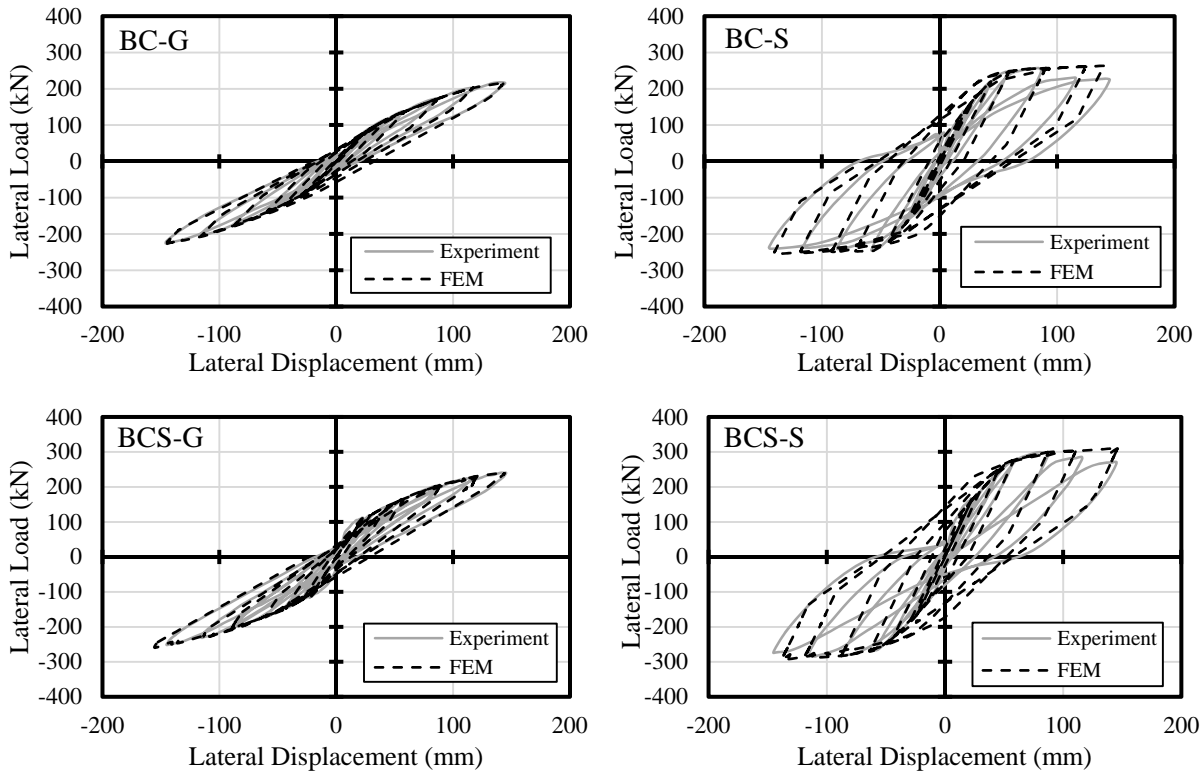


Figure 6. Lateral load-displacement response of beam-column specimens.

RESULTS AND DISCUSSIONS

Frames Corresponding to Beam-Column Specimens

The analysis was performed by direct integration, using Newmark method. The lateral displacement-time response of the first story during the ground excitation for each frame is shown in Figure 7. As shown in the figure, both frames corresponding to the beam-column specimens (BC-S and BC-G) were able to survive the earthquake; however, the maximum lateral displacement of the first story in Specimen BC-G was more than that of Specimen BC-S (117 mm vs. 72 mm). That is due to

the lower modulus of elasticity of GFRP materials compared to steel, which resulted in higher deformations in GFRP-RC frames.

However, it should be mentioned that despite the bigger lateral deformations, the GFRP-RC frame (corresponding to BC-G) exhibited smaller residual displacements compared to the corresponding steel-RC frame (5 mm vs. 9 mm). This is due to the deformability of GFRP-RC beam-columns that allows such elements to achieve big deformations while maintaining their linear elastic nature [5,8].

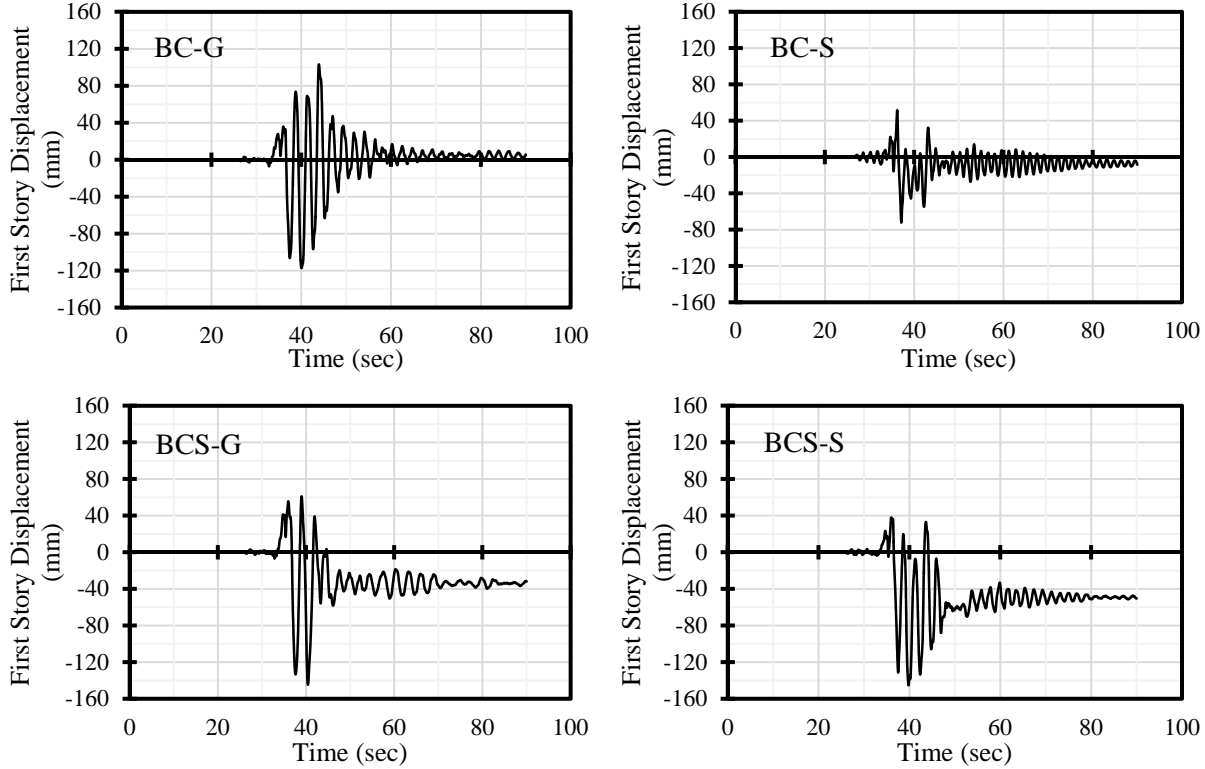


Figure 7. First story lateral displacements.

Table 3 compares the maximum inter-story drift ratio (the drift ratio relative to the immediate lower story) of the frames. The maximum lateral drift ratio allowed by the National Building Code of Canada [18] is 2.5%. As shown in Table 3, the frame corresponding to Specimen BC-G exceeded this limit. However, the lateral drift ratio limits set by the National Building Code of Canada is primarily based on steel-RC structures. Therefore, the 2.5% threshold could be relaxed for GFRP-RC structures as they are capable of withstanding big lateral deformations with insignificant residual damage. However, other restricting factors such as lateral displacement limits to mitigate pounding of adjacent buildings must be appreciated in designing GFRP-RC frames.

Table 3. Maximum inter-story drift ratio.

Specimens	Maximum Drift ratio (%)				
	1 st Story	2 nd Story	3 rd Story	4 th Story	5 th Story
BC-G	3.91	3.28	2.80	1.49	0.77
BC-S	2.40	1.51	1.30	0.98	0.52
BCS-G	4.82	3.40	2.70	1.60	0.89
BCS-S	4.84	2.09	1.56	1.05	0.68

It should be mentioned that bigger deformations in GFRP-RC frames (compared to steel-RC counterparts) could result in excessive bending moment in the columns due to p-delta effect. Therefore, in designing GFRP-RC moment-resisting frames, considerations must be made to account for secondary moments due to p-delta effects.

It is worth mentioning that the maximum drift ratio of the first floor observed in the steel-RC frame (2.4%), which is at the onset of the reinforcement yielding (corresponds to 72 mm in Figure 6), indicating yielding at the base of the modeled building.

Frames Corresponding to Beam-Column-Slab Specimens

The lateral displacement of the first story in the modeled frames corresponding to the beam-column-slab specimens (BCS-S and BCS-G) are also shown in Figure 7. The lateral displacements in both cases are significantly more than their corresponding beam-column specimens. This could be attributed to the higher mass of the beam-column-slab specimens which increased the lateral forces due to ground accelerations.

The higher lateral loads resulted in yielding of the reinforcement in the frame corresponding to Specimen BCS-S, which in turn caused excessive lateral deformations. In contrary to the frames without slabs, the frame for Specimen BCS-G exhibited very similar maximum lateral deformation compared to its steel-RC counterpart. Despite the lower initial lateral stiffness of GFRP-RC frames, they can maintain a constant increase in the lateral load resisting capacities due to their linear nature. Steel-RC frames, on the other hand, exhibit minimal (if any) increase in the lateral load resistance after yielding, which resulted in excessive deformations after yielding.

Moreover, yielding of the reinforcement in the frame corresponding to specimen BCS-S, resulted in significant residual displacement after the seismic event. A 51-mm residual lateral displacement in the first floor of the BCS-S frame was observed, while the magnitude of residual displacement in the counterpart GFRP-RC frame (BCS-G) was measured as 32 mm. This indicates that GFRP-RC frames have the potential of reducing post disaster repair costs by reducing the magnitude of residual damage.

As Table 3 shows, the frames corresponding to the beam-column-slab specimens, showed very similar behaviour in terms of maximum drift ratio of each story to those corresponding to the beam-column specimens. In both cases, the maximum drift ratio decreases in higher stories. However, the decrease is more pronounced in the steel-RC frames.

CONCLUSIONS

According to the results obtained from the analytical study, the following conclusions can be made:

- Lower modulus of elasticity of GFRP reinforcement compared to that of steel (60 GPa vs. 200 GPa) results in bigger lateral deformations of GFRP-RC frames compared to steel-RC counterparts within the elastic range. The modeled frame corresponding to Specimen BC-G (GFRP-RC beam-column) exhibited 63% more lateral deformation in the first floor, compared to its counterpart steel-RC frame, BC-S (steel-RC beam-column). The possible effect of secondary moments (p -delta) due to excessive lateral deformations of GFRP-RC frames must be taken into account during the design process.
- Including the effect of slabs in terms of lateral load-displacement response of beam-column connections and the overall mass of the building, resulted in significant differences in the behaviour of the modeled steel-RC and GFRP-RC frames in terms of lateral deformations and residual damage. Therefore, to accurately evaluate the dynamic performance of moment-resisting frames, the effect of cast-in-situ slabs must be considered.
- Strong lateral forces resulting in yielding of reinforcement in steel-RC moment frames can cause excessive lateral deformations. Despite the higher initial stiffness, the modeled frame corresponding to steel-RC beam-column-slab (BCS-S) exhibited a similar maximum first floor lateral deformation compared to its GFRP-RC counterpart frame (BCS-G). Unlike steel-RC frames that reach a plateau in lateral load carrying capacity after yielding, GFRP-RC frames continue their strength gain up to high lateral drift ratios (5%).
- GFRP-RC frames exhibited less residual damage (displacement), after the seismic loadings, compared to their counterpart steel-RC frames. This indicates that replacing steel reinforcement with GFRP can potentially decrease the post disaster repair costs.

ACKNOWLEDGMENTS

The authors wish to express their gratitude for the financial support received from the Natural Science and Engineering Research Council of Canada (NSERC), through Discovery and Canada Research Chairs programs and the University of Manitoba Graduate Fellowship (UMGF). Also, the authors would like to acknowledge the help received from the technical staff at McQuade Heavy Structures Laboratory at the University of Manitoba.

REFERENCES

- [1] Sharbatdar, M. (2003). "Concrete columns and beams reinforced with FRP bars and grids under monotonic and reversed cyclic loading." Ph.D. thesis, Univ. of Ottawa, Ottawa.
- [2] Tavassoli, A., Liu, J., and Sheikh, S. (2015). "Glass fiber-reinforced polymer-reinforced circular columns under simulated seismic loads." *ACI Struct. J.*, 112(1): 103-114.

- [3] Naqvi, S., and El-Salakawy, E. (2017). "Lap Splice in GFRP-RC Rectangular Columns Subjected to Cyclic-Reversed Loads." *Journal of Composites for Construction*, ASCE, 21 (4), 13 p, 10.1061/(ASCE)CC.1943-5614.0000777.
- [4] Mady, M., El-Ragaby, A. and El-Salakawy, E. (2011). "Seismic Behavior of Beam-Column Joints Reinforced with GFRP Bars and Stirrups." *Journal of Composites for Construction*, ASCE, 15 (6): 875-886.
- [5] Ghomi, S. and El-Salakawy, E. (2016). "Seismic Performance of GFRP-RC Exterior Beam-Column Joints with Lateral Beams." *Journal of Composites for Construction*, ASCE, 20 (1), 11 p, 10.1061/(ASCE)CC.1943-5614.0000582.
- [6] Hasaballa, M.H. and El-Salakawy, E. (2016). "Shear Capacity of Type-2 Exterior Beam-Column Joints Reinforced with GFRP Bars and Stirrups." *Journal of Composites for Construction*, ASCE, 20 (2), 13 p, 10.1061/(ASCE)CC.1943-5614.0000609.
- [7] Ghomi, S. and El-Salakawy, E. (2018). "Seismic Behaviour of Exterior GFRP-RC Beam-Column Connections: Analytical Study." *Journal of Composites for Construction*, 22(4), 13p, 10.1061/(ASCE)CC.1943-5614.0000858.
- [8] Ghomi, S. and El-Salakawy, E. (2018). "Seismic Performance of Interior GFRP-RC Beam-Column Joints." *ACI Special Publication*, Farmington Hills, Detroit, Michigan, 2018, 20 p.
- [9] Duggal, S. (2013). "Earthquake Resistant Design of Structures (2nd Edition)." Oxford University Press, 528 p.
- [10] CSA. (2012). "Design and construction of building components with fibre reinforced polymers." CAN/CSA-S806-12, Canadian Standards Association Ontario, Canada, 206 p.
- [11] ACI Committee 440. (2015). "Guide for Design and Construction of Concrete Reinforced with FRP Bars." ACI 440.1R-15, American Concrete Institute, Farmington Hills, Mich., 44 p.
- [12] CSI. (2016). "CSI Analysis Reference Manual for SAP2000, ETABS, SAFE and CSiBridge." Computers and Structures Inc., California, USA, 206 p.
- [13] Ehsani, M., R. and Wight, J. K. (1985-b). "Effect of Transverse Beams and Slabs on Behaviour of Reinforced Concrete Beam-to-Column Connections." *ACI Structural Journal*, 82(17): 188-195.
- [14] Zerbe, H., E. and Durrani, A., J. (1990). "Seismic Response of Connections in Two-Bay Reinforced Concrete Frame Subassemblies with a Floor Slab." *ACI Structural Journal*, 87(4): 406-415.
- [15] Ning, N., Qu, W. and Zhu, P. (2014). "Role of Cast-in Situ Slabs in RC Frames under Low Frequency Cyclic Load." *Engineering Structures*, V. 59: 28-38.
- [16] Pultrall Inc., V.ROD Canada, GFRP Specification Guide, Available at <http://www.vrodcanada.com/product-data/gfrp-specification-guide>, visited on December 21, 2018.
- [17] ACI Committee 374. (2005). "Acceptance Criteria for Moment Frames Based on Structural Testing and Commentary." ACI 374.1-05, American Concrete Institute, Farmington Hills, MI, 88 p.
- [18] NRCC. (2015). "National Building Code of Canada (NBCC)." National Research Council of Canada, Ottawa, Ontario, 1245 p.